frontiers | Frontiers in Immunology

TYPE Brief Research Report
PUBLISHED 20 March 2025
DOI 10.3389/fimmu.2025.1501329

OPEN ACCESS

EDITED BY
Juraj Ivanyi,
King's College London, United Kingdom

REVIEWED BY
Marco Pio La Manna,
University of Palermo, Italy
Nathan Scott Kieswetter,
University of Washington, United States

*CORRESPONDENCE
Theodoros Karantanos
tkarant1@jhmi.edu
Styliani Karanika
skarani1@jhmi.edu

†These authors have contributed equally to this work and share first authorship

‡These authors have contributed equally to this work and share last authorship

RECEIVED 24 September 2024
ACCEPTED 28 February 2025
PUBLISHED 20 March 2025

CITATION
Wang T, Quijada D, Ahmedna T, Castillo JR, Naji NS, Peske JD, Karakousis PC, Paul S, Karantanos T and Karanika S (2025) Targeting CCRL2 enhances therapeutic outcomes in a tuberculosis mouse model. *Front. Immunol.* 16:1501329. doi: 10.3389/fimmu.2025.1501329

Targeting CCRL2 enhances therapeutic outcomes in a tuberculosis mouse model

Tianyin Wang[1,2†], Darla Quijada[1,2†], Taha Ahmedna[3], Jennie Ruelas Castillo[1,2], Nour Sabiha Naji[4], J David Peske[5], Petros C. Karakousis[1,2], Suman Paul[3,5], Theodoros Karantanos[4*‡] and Styliani Karanika[1,2*‡]

[1]Division of Infectious Diseases, Department of Medicine, The Johns Hopkins Hospital, Baltimore, MD, United States, [2]Center for Tuberculosis Research, Department of Medicine, Johns Hopkins University School of Medicine, Baltimore, MD, United States, [3]Ludwig Center and Lustgarten Laboratory, Sidney Kimmel Comprehensive Cancer Center, The Johns Hopkins University School of Medicine, Baltimore, MD, United States, [4]Division of Hematologic Malignancies, Department of Medical Oncology, The Johns Hopkins University School of Medicine, Baltimore, MD, United States, [5]Division of Hematopathology, Department of Pathology, The Johns Hopkins University School of Medicine, Baltimore, MD, United States

Tuberculosis (TB) remains among the leading infectious causes of death. Due to the limited number of antimicrobials in the TB drug discovery pipeline, interest has developed in host-directed approaches to improve TB treatment outcomes. C-C motif chemokine-like receptor 2 (CCRL2) is a unique seven-transmembrane domain receptor that is upregulated by inflammatory signals and mediates leucocyte migration. However, little is known about its role in TB infection. Here, we show that *Mycobacterium tuberculosis* (Mtb) infection increases CCRL2 protein expression in macrophages *in vitro* and alveolar macrophages (AMs), dendritic cells (DCs) and neutrophils in mouse lungs. To target selectively CCRL2-expressing cells *in vivo*, we developed a novel mouse anti-CCRL2 antibody-drug conjugate (ADC) linked with the cytotoxic drug SG3249. We tested its adjunctive therapeutic efficacy against TB when combined with the first-line regimen for drug-susceptible TB (isoniazid, rifampin, pyrazinamide, ethambutol; RHZE). The anti-CCRL2 ADC treatment potentiated RHZE efficacy in Mtb-infected mice and decreased gross lung inflammation. CCRL2 expression in lung DCs and AMs was lower in mice receiving anti-CCRL2 ADC treatment +RHZE compared to those receiving RHZE alone or the control group, although the total innate cell populations did not differ across treatment groups. Interestingly, neutrophils were completely absent in the anti-CCRL2 ADC treatment + RHZE group, unlike in the other treatment groups. IFN-γ+-and IL17-α+-T-cell responses, which are associated with optimal TB control, were also elevated in the anti-CCRL2 ADC treatment + RHZE group. Our findings suggest that CCRL2-targeting approaches may improve TB treatment outcomes, possibly through selective killing of Mtb-infected innate immune cells.

KEYWORDS

CCRL2, TB, antibody-drug conjugate, dendritic cells, alveolar macrophages, neutrophils, adjunctive therapeutic treatment

Introduction

Tuberculosis (TB) remains one of the leading infectious causes of death worldwide (1). The currently available six-month regimen consisting of isoniazid, rifampin, pyrazinamide, and ethambutol (collectively, RHZE) is highly effective against drug-susceptible TB. However, its length and complexity leads to treatment interruptions that adversely affect cure rates and increase the incidence of drug resistance (2, 3). Thus, novel approaches that can shorten the duration of TB drug treatment are urgently needed to improve patient clinical outcomes.

Due to the limited number of antimicrobials in the TB drug discovery pipeline, host-directed strategies have generated considerable interest (4). Host immunity plays a critical role in the outcomes of TB disease (5). *Mycobacterium tuberculosis* (Mtb) has developed several evasion strategies, prompting the host to elicit an immune response that favors its persistence (5). Host-directed strategies targeted at "re-educating" the immune system are realistic alternative approaches to tailor the host response against TB (5).

Neutrophils, macrophages, and dendritic cells (DCs) are among the major innate immune cell types involved in Mtb infection (6–8). Although they are intended to target the invading pathogen, they may facilitate immune surveillance escape (7–9). Mtb-infected alveolar macrophages (AMs) have poor bactericidal capabilities and show immunoregulatory features suppressing lymphocyte activation (10). Similarly, Mtb antigens alter differentiation, suppress maturation, and induce the expression of inhibitory molecules in DCs, suppressing their activity (11, 12). Neutrophils display weak antimycobacterial activity and may promote mycobacterial survival through immune surveillance escape (7). Neutrophil degranulation, which is meant to target Mtb, may also cause the destruction of neighboring cells and tissue dissolution (9, 13). Thus, further investigation of the molecular and cellular alterations mediating the phenotypic changes of these cells can improve our understanding of TB pathogenesis. Targeting molecules halting these alterations could be a promising approach to enhance the efficacy of currently available anti-TB therapies.

C-C motif chemokine-like receptor 2 (CCRL2) is a seven-transmembrane domain receptor that is upregulated by inflammatory signals (14). It does not promote chemotaxis but mediates leukocyte migration (14, 15). CCRL2 has been recently found to promote malignant cell growth in myelodysplastic syndrome and secondary acute myeloid leukemia (16), while its deletion increased the sensitivity of these cells to azacytidine, a first-line chemotherapy for these malignancies (17). Data on the potential role of CCRL2 in TB are scarce. Petrilli et al. applied an immune-based gene expression profile and found that CCRL2 was one of the 7 genes that can predict the progression of latent TB infection to TB disease with high sensitivity and specificity (18). Consistently, silencing of CCRL2 abolished Mtb-induced macrophage M2 polarization, a phenotype associated with a suppressive microenvironment promoting Mtb intracellular growth (19).

In this study, we show that Mtb infection increases the expression of CCRL2 *in vitro* and *in vivo* (lung-derived DCs, AMs and neutrophils) and targeting CCRL2 with an antibody-drug conjugate (ADC) potentiates the bactericidal activity of RHZE in a mouse TB model, suggesting that this approach may be a promising adjunctive TB therapeutic tool.

Materials and methods

Bacteria

Wild-type and green fluorescent protein (GFP+)-expressing Mtb H37Rv was grown in Middlebrook 7H9 broth (Difco, Sparks, MD) supplemented with 10% oleic acid-albumin-dextrose- catalase (OADC, Difco), 0.2% glycerol, and 0.05% Tween-80 at 37°C in a roller bottle (20).

Cell line and *in vitro* reagents

Human THP1 cells were purchased from the American Type Culture Collection and cultured in RPMI-1640 with 10% heat-inactivated fetal bovine serum (hiFBS) with 2 mM l-glutamine, penicillin (100 U/ml), and streptomycin (100 µg/ml) at 37°C in 5% CO_2. Phorbol 12-myristate 13-acetate (PMA) was purchased from Sigma-Aldrich (#P1585-5MG).

Mtb infection *in vitro*

THP1 cells were maintained in RPMI 1640 supplemented with 10% hiFBS. Cells were differentiated with 50ng/ml PMA for 48 hours, washed, rested overnight with media containing no PMA, and infected in a growth medium containing 5% human serum. GFP+ bacteria were added to cells at a multiplicity of infection (MOI)= 1 or 10 for 1 or 2 days at 37°C, and extracellular bacteria were removed by sequential washes with PBS. Cells were then stained and analyzed by flow cytometry.

Generation and analysis of antibody-drug conjugates

The anti-CCRL2 (BioLegend #114002 and #358304) and IgG2b (BioLegend # 400602 and 400608) mouse and human monoclonal antibodies were partially reduced using 5 molar excess Tris(2-carboxyethyl) phosphine hydrochloride (TCEP, Thermo Fisher Scientific, #77720) for 2 hours at 37°C with rotation, followed by TCEP removal by buffer exchange into PBS using Zeba Spin 7-kDa molecular weight cut-off (MWCO) columns. The SG3249 (Med Chem Express #HY-128952) solution was prepared by resuspending SG3249 in DMSO stock solution at 10 mM

concentration. The SG3249 working solution was prepared by diluting the stock solution in sufficient DMSO to make the final conjugation reaction mixture 10% organic and 90% aqueous. This solution was added to the partially reduced antibodies at fivefold molar excess and incubated for 2 hours at room temperature with rotation. The excess unreacted drug linkers were removed by buffer exchange into PBS using Zeba Spin 7 kDa MWCO columns. The ADCs were analyzed for concentration using the Pierce BCA Protein Assay (Thermo Fisher Scientific, #23227), and drug–antibody conjugation and the presence of the residual free drug by high-performance liquid chromatography (HPLC) as previously described (21, 22).

Mouse Mtb infections

All *in vivo* procedures were performed according to protocols approved by the Johns Hopkins University Institutional Animal Care and Use Committee. Four-to-six-week-old male and female C57BL6 mice were purchased from The Jackson Laboratory. The mice were housed in individually ventilated cages maintained on a 12:12h light/dark cycle with free access to food and water. They were monitored at least weekly, recording their weights and assessing their general appearance. They were infected between 6 and 8 weeks of age with ~100 bacilli of wild-type Mtb H37Rv via the aerosol route using the Glas-Col Inhalation Exposure System (Terre Haute, IN), and this procedure did not require anesthesia. On the day after infection, at least 5 mice per experiment were sacrificed to determine the number of colony-forming units (CFUs) implanted into the lungs.

Mouse antibiotic treatments

When applicable, after 28 days of infection, at least 5 animals per experiment were sacrificed to determine the CFUs present in the lungs at the start of treatment. On the same day, the mice were randomized to receive either human-equivalent doses of H (10 mg/kg), R (10 mg/kg), Z (150 mg/kg), and E (100 mg/kg) dissolved in distilled water or distilled water only (control group) (23). The Z solution was gently heated in a 55°C water bath and vortexed to dissolve before treating mice. To minimize drug-drug interactions, R was administered at least 1 hour before Z. All drugs were administered once daily, by orogastric gavage, in a total volume of 0.2-0.3 ml/mouse/day.

Mouse ADC treatments

Seven weeks after the Mtb aerosol infection, the CCRL2 and its isotope IgG control ADC were administered once, at a dose of 0.75 mg/kg, through a lateral tail vein injection using an insulin syringe with a 28-gauge needle. The needle was bent at an angle of 30–50°. The total volume did not exceed 100 µl. Animals were warmed under a heating lamp to promote vasodilatation for less than 30 seconds, and the needle was placed on the surface almost parallel to the vein and inserted carefully.

Tissue collection and bacterial enumeration

Mice were sacrificed 7 weeks after drug treatment initiation (CCRL2 ADC experiment) or 16 weeks after Mtb infection (CCRL2 expression in Mtb-infected vs. uninfected mice). Right lower lungs were harvested and processed into single-cell suspensions after mechanical disruption and filtration through a 70-µm cell strainer and then additionally digested using collagenase Type I (ThermoFisher Scientific) and DNase (Sigma-Aldrich) for 20 min at 37°C (20). Single-cell suspensions were resuspended in warm R10 (RPMI 1640 with 2 mM-glutamine, 100 U ml^{-1} penicillin, 100 µg ml^{-1} streptomycin, 20mM HEPES, 1% sodium pyruvate, 1% non-essential amino acids and 10% hiFBS; Atlantic Biologicals) for flow cytometry analysis, as detailed below. The right upper lung of each mouse was homogenized using glass homogenizers for bacterial burden assessment. Serial tenfold dilutions of lung homogenates in PBS were plated on 7H11 selective agar (BD) supplemented with 50µg/ml Cycloheximide, 50µg/ml Carbenicillin, 25µg/ml Polymixin B, and 20µg/ml Trimethoprim for CFU enumeration. Plates were incubated at 37°C, and CFU were counted 4 weeks later by at least 2 investigators (20). The left lung was fixed by immersion in 10% neutral buffered formalin for at least 48 hours, paraffin-embedded, and sectioned for immunohistochemical analysis.

Immunohistochemical analyses

Following the preparation of paraffin lung sections, slides were prepared and stained using hematoxylin and eosin (H&E). The degree of lung inflammation was quantified by measuring integrated density using the Image J software in various lung fields, at least 3 per mouse per group, by 2 investigators.

Multiparameter flow cytometry

$1x10^6$ THP-1 cells seeded for each replicate. Cells were collected with trypsin-EDTA and incubated for 5 minutes in the incubator (5% CO_2 at 37°C). Cells were resuspended in FACS buffer (PBS + 0.5% Bovine serum albumin (Sigma-Aldrich, St. Louis, MO) and stained with FcX Blocker for 5 minutes at room temperature. Then, it was stained with Zombie NIR Fixable Viability Kit for 15 minutes at room temp. Then, cell surface staining with the following anti-human antibodies: PE-conjugated anti-CCRL2 (Biolegend #358304), APC-conjugated anti-CD14 (Biolegend #325607), BV421-conjugated anti-CD11b (Biolegend #393113) for 30 minutes. Cells were fixed with 4% PFA for 30 minutes and then washed and resuspended with FACS buffer (PBS + 0.5% Bovine serum albumin (Sigma-Aldrich, St. Louis, MO). Single-cell suspensions from mouse lungs were prepared as above. For Intracellular Cytokine Staining (ICS), GolgiPlug cocktail

(BD Pharmingen, San Diego, CA) was added for 4 hours, and cells were collected using FACS buffer (PBS + 0.5% Bovine serum albumin (Sigma-Aldrich, St. Louis, MO). Intracellular proteins were stained for 20 minutes, and samples were washed, fixed, and resuspended with FACS buffer. The following anti-mouse mAbs were used for ICS: PercPCy5.5 conjugated anti-CD3 (Biolegend Cat. No 100217), FITC-conjugated anti-CD4 (Biolegend Cat. No 100405), Alexa Fluor 700 conjugated anti-CD8 (Biolegend Cat. No. 155022), APC conjugated anti-IFN-γ, (Biolegend Cat. No. 505809), PE-conjugated anti-IL-17α (Biolegend Cat. No 506903), BUV563-conjugated anti-CD19 (BD Biosciences Cat. No. 749028), BUV496-conjugated anti-NK-1.1 (BD Biosciences Cat. No. 741062), BV605-conjugated anti-Ly-6G (Biolegend Cat. No. 127639), BV421-conjugated anti-CD11c (Biolegend Cat. No. 117330), BV650-conjugated anti-CD64 (Biolegend Cat. No. 104732), BUV805-conjugated anti-CD11b (BD Biosciences Cat. No. 741934), BV510-conjugated anti-MHCII (Biolegend Cat. No. 107636), FITC-conjugated anti-CD103 (Biolegend Cat. No. 121420). BD Biosciences LSRII/Fortessa flow cytometers were used. Flow data were analyzed by FlowJo Software (FlowJo 10.9, LLC Ashland, OR). The two-dimensional gating strategy for flow cytometric identification of T-cell-producing cytokines and DCs, alveolar macrophages, and neutrophils is shown in Supplementary Figure 3.

Statistics

All reported P values are from two-sided comparisons. Pairwise comparisons of group mean values for $\log_{10}$ CFU (microbiology data) and flow cytometry data were made using a one-way analysis of variance followed by Tukey's multiple comparisons test or unpaired T-test. All error bars represent the estimation of the standard error of the mean, and all midlines represent the group mean unless otherwise specified. Prism 9.3 (GraphPad Software, Inc. San Diego, CA) was utilized for statistical analyses and figure generation. A significance level of $\alpha \leq 0.05$ was set for all experiments.

Results

Mtb infection increases CCRL2 protein expression *in vitro* and *in vivo*

To evaluate the effect of Mtb infection on CCRL2 expression in macrophages *in vitro*, THP-1 cells were infected with a GFP +-expressing Mtb strain following treatment with PMA to induce differentiation to macrophages (Figure 1A). Uninfected THP-1 cells

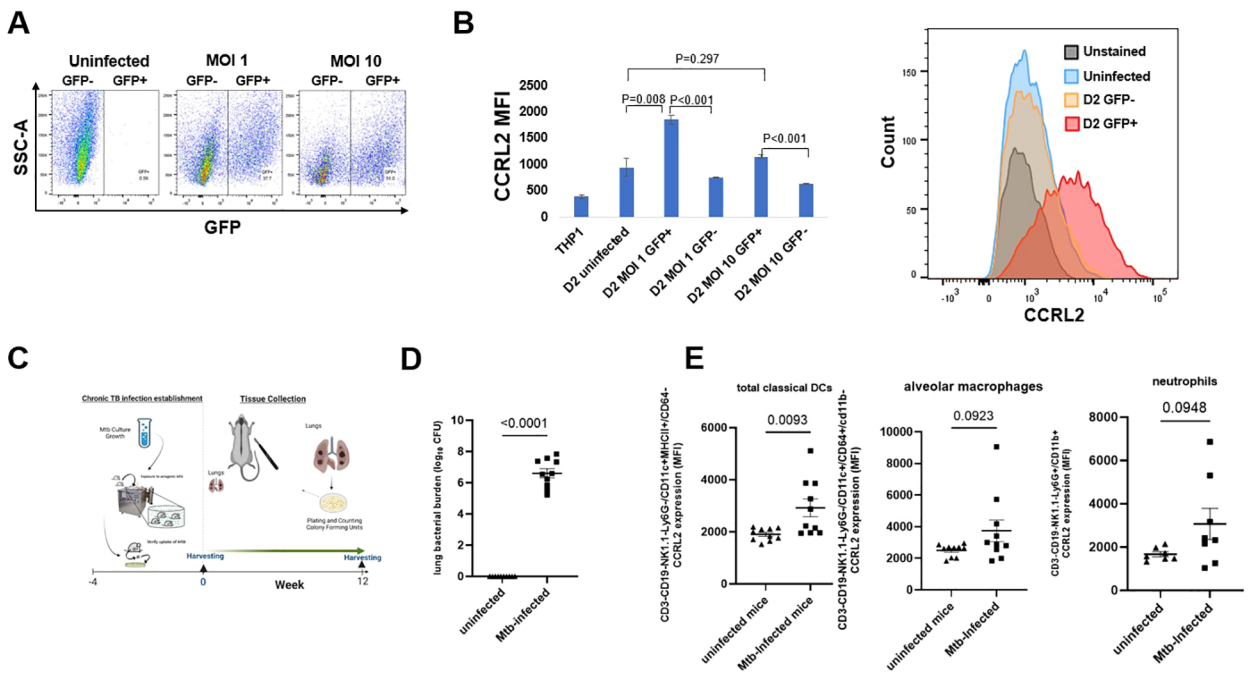

FIGURE 1
Mtb infection increases CCRL2 protein expression *in vitro* and *in vivo*. **(A, B)** THP-1 cells were infected with the GFP+ Mtb strain at MOI of 1 and 10 following treatment with PMA to induce differentiation to macrophages and were incubated for 2 days. Using flow cytometry, CCRL2 expression (MFI) was measured across the different conditions; This experiment was repeated three times, and a one-way analysis of variance followed by Tukey's multiple comparisons tests was used; **(C)** Timeline of Mtb challenge study **(D)** Lung mycobacterial burden between uninfected mice (n=10) and Mtb infected mice (n=9) at 16 weeks (end of experiment); unpaired T-test was used; and **(E)** CCRL2 expression of lung-derived classical DCs, alveolar macrophages and neutrophils collected from Mtb-infected at 16-week timepoint vs. uninfected mice. Flow cytometry experiments was repeated at least twice, and unpaired T-test was used; MOI, Multiplicity of infection; GFP, green fluorescent protein; D2, Day 2; MFI, Median fluorescent intensity; Mtb, Mycobacterium tuberculosis, CFU, colony-forming units; Classical DCs, classical dendritic cells.

were also included as controls. CD11b+ and CD14+ expression (measured as median fluorescent intensity) were used to confirm differentiation of THP-1 treated with PMA (Supplementary Figure 1A). CCRL2 expression was significantly upregulated in alive Mtb-infected THP-1 cells compared to uninfected or GFP- cells on day 1 (P=0.023 between MOI 10 GFP+ vs. GFP- cells) (Supplementary Figure 1B) and day 2 (P<0.001 between MOI 1 and 10 GFP+ vs. GFP- cells) (Figure 1B).

Next, to validate our *in vitro* findings, we sought to measure CCRL2 expression in the lungs of Mtb-infected and uninfected C57BL6 male and female mice. Sixteen weeks after infection, the lungs were collected (Figure 1C), and uninfected mice of similar age were used as controls (Figure 1D). CCRL2 expression was significantly higher in classical DCs in the lungs of infected mice compared to those of uninfected mice (P=0.009). A similar trend was also found in CCRL2 expression in alveolar macrophages (P=0.0923) and neutrophils (P=0.0948) (Figure 1E). We show the respective cell populations, expressed in percentages, in Supplementary Figure 1C, where no substantial differences were noted between infected vs. uninfected mice.

Treatment with an anti-CCRL2 ADC potentiates the activity of RHZE and decreases gross lung inflammation

Next, to investigate the effect of CCRL-2 deletion on TB treatment outcomes *in vivo*, we tested the adjunctive therapeutic efficacy of an anti-CCRL2 ADC when combined with the first-line regimen for drug-susceptible RHZE. The mouse anti-CCRL2 ADC was generated by conjugating the commercially available anti-mouse CCRL2 antibody with the cytotoxic DNA minor groove inter-strand pyrrolobenzodiazepine dimer SG3249. An anti-mouse rat IgG2b was conjugated with SG3249 as an isotope control. The conjugation was confirmed by HPLC (Figure 2A, Supplementary Figure 2A).

C57BL/6 mice were aerosol-infected with Mtb, and 4 weeks later, antibiotic treatment with RHZE was initiated (Figure 2B). Three weeks later, the mice were intravenously treated with one dose (0.75 mg/kg) of the anti-CCRL2 ADC or the isotope control, anti-IgG ADC. Mice were sacrificed 4 weeks later to assess lung mycobacterial burden (Figure 2B). The lung bacterial burden was found to be significantly lower in mice treated with anti-CCRL2 ADC + RHZE compared to those treated with the RHZE + isotope control (P<0.0001) or RHZE alone (P<0.0001) (Figure 2C). No difference in therapeutic adjunctive benefit was noted between males and females. The mouse lung-to-body weight ratio, an index reflective of gross lung inflammation, was significantly lower in mice treated with the anti-CCRL2 ADC than those treated with the anti-IgG ADC (P<0.0001) or RHZE alone (P<0.0001) (Figure 2C). The spleen bacterial burden was not found to be significantly different between mice treated with anti-CCRL2 ADC + RHZE compared to those treated with the RHZE + isotope control (P=0.1564). Still, it was close to reaching statistical significance when compared with RHZE alone (P=0.0541)

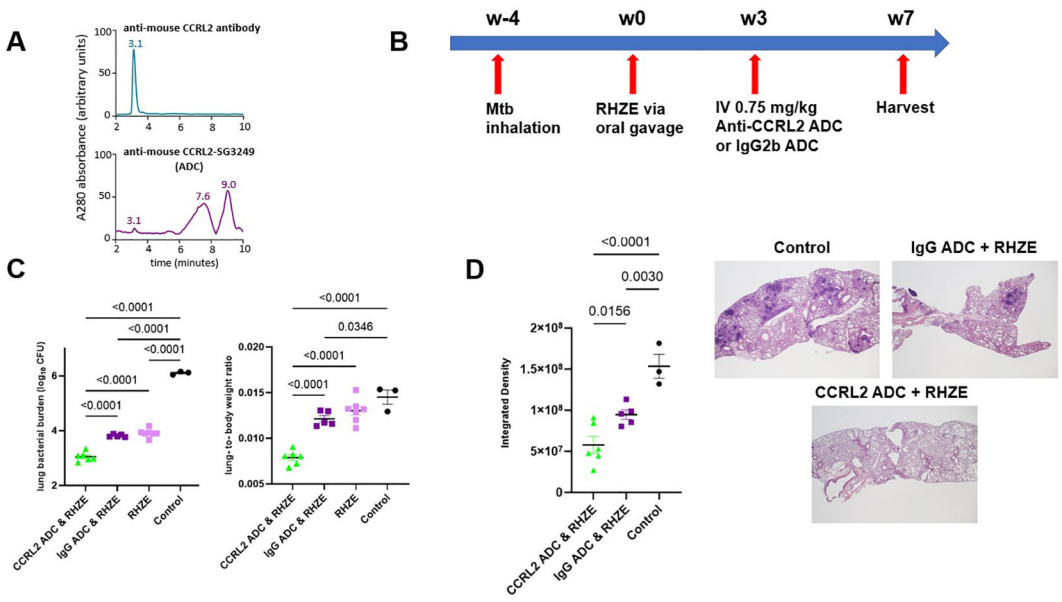

FIGURE 2
Treatment with an anti-CCRL2 ADC potentiates the activity of RHZE and decreases gross lung inflammation **(A)** Hydrophobic interaction chromatography (HPLC) of anti-CCRL2 antibody and anti-CCRL2-SG3249 ADC; **(B)** Timeline of the Mtb challenge study; **(C)** Scatterplot of lung mycobacterial burden in mice (n=20) and lung-to body-weight ratio at 7 weeks after RHZE; **(D)** Scatterplot of integrated density, as measure of gross lung inflammation, in at least 3 lung fields/mouse/group, across the different treatment groups (n=14) and representative H & E slides per group. This experiment was conducted once, and one-way analysis of variance followed by Tukey's multiple comparisons tests was used; Mtb, Mycobacterium tuberculosis, RHZE, Rifampin-Isoniazid-Pyrazinamide-Ethambutol; ADC, Antibody-drug conjugate; CFU, colony-forming units; IgG ADC, isotype control IgG2b-SG3249 ADC.

(Supplementary Figure 2B). Of note, no toxicity was appreciated during the study in any treatment group as measured by weight gain (Supplementary Figure 2C) or other signs of morbidity or mortality, including premature deaths (none reported in any experimental group). Similarly, inflammation was also evaluated histopathologically. Lung inflammation, as measured by the surface area containing inflammatory lesions obliterating the lung parenchyma (integrated density), was significantly reduced in mice treated with adjunctive anti-CCRL2 ADC compared to those treated with the anti-IgG ADC (P=0.015) (Figure 2D).

Treatment with anti-CCRL2 ADC lowers CCRL2 expression in innate immune cells and induces TB-protective immune responses

To gain insight into the potential mechanisms underlying the adjunctive therapeutic efficacy of the anti-CCRL2 ADC, we measured the CCRL2 expression in innate immune cells derived from the lungs of mice receiving each of the different treatment groups using flow cytometry. We found that mice treated with anti-CCRL2 ADC + RHZE had non-significantly lower CCRL2 expression (expressed in median fluorescent intensity) in lung classical DCs 1 (P=0.2366) and DCs 2 (P=0.0772) and alveolar macrophages (P=0.076) compared to those treated with the anti-IgG ADC + RHZE (Figure 3A). Interestingly, the populations (%) of classical DCs 1 and 2 and alveolar macrophages isolated from the lungs of mice treated with anti-CCRL2 ADC + RHZE either were relatively increased or did not have significant variation compared to the IgG ADC + RHZE group (P=0.3716, 0.1390, 0.0895, respectively) (Figure 3B). Notably, the neutrophils isolated from the lungs of mice treated with anti-CCRL2 ADC + RHZE were undetectable in contrast to the IgG ADC + RHZE or control group (P=0.0062 and <0.0001, respectively) (Figure 3B). Taken together, these findings suggest that the adjunctive therapeutic efficacy of the CCRL2 ADC treatment may be associated with lower CCRL2 expression by DCs and alveolar macrophages, as well as a dramatic reduction of neutrophils.

Finally, we measured the T-cell immune responses associated with optimal TB control in the murine lungs (24–27). The percentage of CD4+ and CD8+ T cells producing IFN-γ and CD4 + T cells producing IL17-A were either relatively or significantly increased in the lungs of mice receiving anti-CCRL2 ADC + RHZE compared to those receiving anti-IgG ADC + RHZE (P=0.0122, P=0.078, and P=0.0305, respectively) (Figure 3C).

Discussion

In this work, we show that CCRL2, a unique non-signaling seven-transmembrane domain receptor known to be upregulated in inflammatory signals (14–16, 19), may play an important role in TB pathogenesis. Specifically, we found that CCRL2 expression is

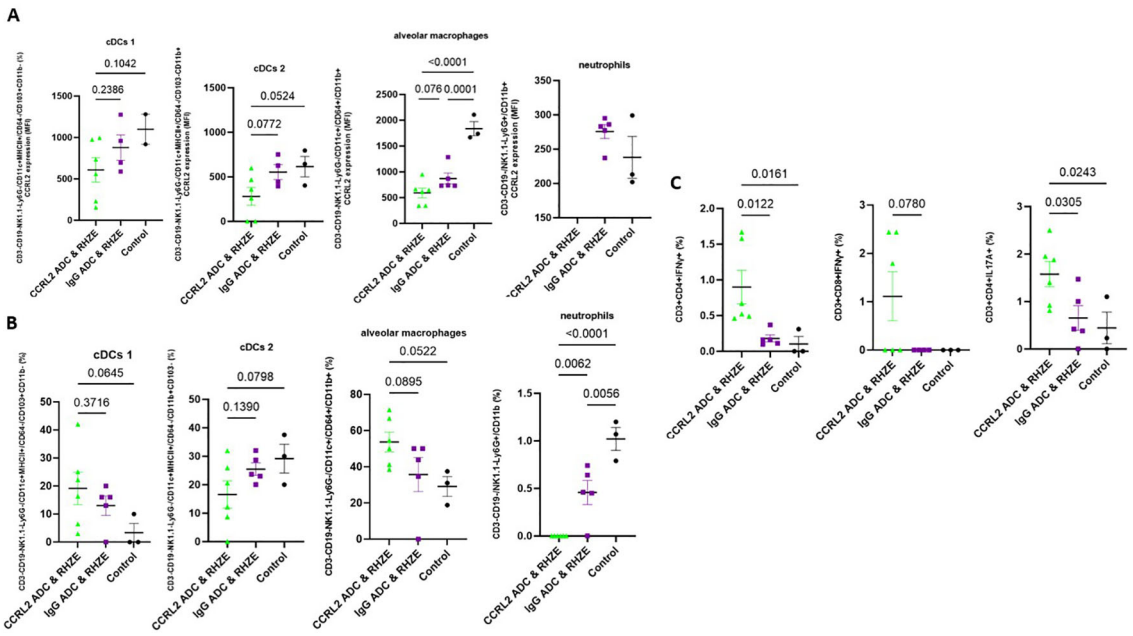

FIGURE 3
Treatment with an anti-CCRL2 ADC lowers CCRL2 expression in innate immune cells and induces TB-protective immune responses. **(A)** CCRL2 expression (MFI) in cDCs 1, cDCs 2, alveolar macrophages and neutrophils derived from mouse lungs across the different treatment groups; CCRL2 expression in neutrophils derived from mice receiving CCRL2 ADC & RHZE is not shown since neutrophil count in that group was 0; **(B)** populations (%) of cDCs 1, cDCs 2, alveolar macrophages and neutrophils derived from mouse lungs across; **(C)** IFNγ-CD4+ and CD8+ T cell producing cells and IL17α-CD4+ T cell producing cells (%) across the different groups; Assessment was performed using flow cytometry and experiments repeated at least twice. One-way analysis of variance followed by Tukey's multiple comparisons tests was used; RHZE, Rifampin-Isoniazid-Pyrazinamide-Ethambutol; cDCs I, classical dendritic cells type I; cDCs II, classical dendritic cell type 2; ADC, antibody-drug conjugate. MFI, median fluorescent intensity.

increased in Mtb-infected differentiated THP-1 cells and higher in lung-derived DCs and alveolar macrophages in Mtb-infected mice compared to uninfected mice. Targeting CCRL2 using an anti-CCRL2 ADC offered adjunctive therapeutic activity in Mtb-infected mice when combined with the first-line TB regimen. Anti-CCRL2 ADC treatment lowered CCRL2 expression by lung DCs and alveolar macrophages and abolished lung neutrophils. It also induced local TB-protective T-cell responses, suggesting that this novel host-directed therapy may be a promising therapeutic tool.

The role of CCRL2 in immunity is not clearly described. It is suggested that it responds to inflammatory signals, and one of the proposed mechanisms of action involves the formation of heterodimers with chemokine receptors (15). Heterodimerization of chemokine receptors is a potentially crucial step for the proper function of immune cells (28, 29). In particular, CCRL2/CXCR2 heterodimers control neutrophil recruitment in inflammatory arthritis (15), resulting in protection in CCRL2-deficient mice (15, 30). Similarly, CCRL2 expression is upregulated in synovial neutrophils of patients with rheumatoid arthritis compared to healthy controls (31). In an allergen-induced airway inflammation model, where DCs are known to play a crucial role (32), CCRL2 deficiency impaired DC migration, leading to an adaptive immune response defect, which was abrogated with adoptive transfer of wild-type DCs (33). Silencing of CCRL2/CX3CR1 abolished Mtb-induced macrophage M2 polarization, a cell population associated with Mtb growth (19). Combining all the available evidence, we hypothesized that TB, as an inflammatory disease, promotes CCRL2 expression. Indeed, we found that CCRL2 expression is higher in Mtb-infected differentiated THP-1 cells, which was also confirmed *in vivo*. Adjunctive treatment with the novel targeted therapy anti-CCRL2-ADC further reduced the lung bacillary burden *in vivo*.

ADCs have been developed and successfully introduced in clinical practice as disease-selective treatments for various types of cancer, particularly hematologic malignancies (22, 34–36). The delivery of the toxic drug selectively to cells expressing a surface marker allows disease-specific therapy while sparing other cells. CCRL2 is expressed at very low levels in healthy hematopoietic stem and progenitor cells (16) and at low levels in healthy non-inflamed tissues (15, 37). Of note, global deficiency of CCRL2 did not alter normal development and had no significant impact on blood counts or incidence of infection in mouse models (15, 38). These findings render CCRL2 an attractive and safe target for selective therapies, including our novel anti-CCRL2 ADC, which had no associated toxicity when tested *in vivo*. Upon binding to the target (CCRL2), the toxin is released inside CCRL2-expressing cells and causes DNA minor groove cross-links. The latter increases replication fork stalling, causing induction of apoptosis.

One possible mechanism of action of our anti-CCRL2 ADC is by selectively killing Mtb-infected innate immune cells, which contribute to immune surveillance escape. Indeed, we observed lower CCRL2 expression in lung DCs and alveolar macrophages of mice receiving the anti-CCRL2 ADC + RHZE, which was accompanied by the lowest lung mycobacterial burden compared to the anti-IgG ADC + RHZE or control groups, although the total population of DCs or alveolar macrophages was either unchanged or higher in the former group. Also, we observed that the neutrophil population was completely abolished in the anti-CCRL2 ADC + RHZE mouse group, suggesting that neutrophils are major contributors to the TB-associated inflammatory response and express CCRL2 targeted by the novel anti-CCRL2 ADC. This is not surprising since neutrophilia is independently associated with an increased risk of cavity formation, lung tissue damage, and mortality in patients undergoing TB therapy, suggesting that the neutrophil count in TB positively correlates with bacillary load and disease outcome (39, 40).

Our study has some limitations. Although our findings allow us to make some initial associations between the adjunctive therapeutic role of the anti-CCRL2 ADC treatment and CCRL2 expression in the innate immune cells, further studies are needed to elucidate the mechanism of action in the TB setting. Also, follow-up studies evaluating the potential of shortening the curative TB treatment are imperative. Last, additional studies are needed to test the therapeutic efficacy of this novel intervention in other animal models that more closely represent human TB pathology.

In conclusion, our data suggests that Mtb infection increases CCRL2 expression, and CCRL2-targeting approaches may improve TB treatment outcomes, possibly through selective killing of innate immune cells harboring Mtb. Ultimately, the potential utility of this novel strategy must be evaluated as an adjunctive therapeutic intervention in shortening the duration of curative treatment for active TB.

Data availability statement

The original contributions presented in the study are included in the article/Supplementary Material. Further inquiries can be directed to the corresponding author/s.

Ethics statement

The animal study was approved by Johns Hopkins Animal Care and Use Committee. The study was conducted in accordance with the local legislation and institutional requirements.

Author contributions

TW: Data curation, Formal analysis, Investigation, Methodology, Visualization, Writing – review & editing, Validation. DQ: Data curation, Formal analysis, Investigation, Methodology, Validation, Visualization, Writing – review & editing. TA: Data curation, Investigation, Methodology, Writing – review & editing, Visualization. JC: Formal analysis, Investigation, Methodology, Writing – review & editing. NN: Writing – review & editing, Formal analysis, Investigation, Methodology. JP: Data curation, Formal analysis, Investigation, Methodology, Supervision, Visualization, Writing – review & editing. PK: Supervision, Writing – review & editing, Funding acquisition, Resources. SP: Funding acquisition, Resources, Supervision, Writing – review & editing,

Conceptualization, Data curation, Formal analysis, Investigation, Methodology, Software, Validation. TK: Conceptualization, Data curation, Formal analysis, Funding acquisition, Investigation, Methodology, Resources, Supervision, Validation, Project administration, Software, Visualization, Writing – original draft. SK: Conceptualization, Data curation, Formal analysis, Funding acquisition, Investigation, Methodology, Project administration, Resources, Software, Supervision, Validation, Visualization, Writing – original draft.

Funding

The author(s) declare that financial support was received for the research and/or publication of this article. This work was supported by NIH grants: K08AI174959 (SK), K08HL168777 (TK), K08CA270403 (SP), R01AI148710 (PCK), K24AI143447 (PCK), P30AI168436 (PCK). The content is solely the responsibility of the authors and does not necessarily represent the official views of the National Institutes of Health. SK was also supported by the Johns Hopkins CFAR developmental award (5P30AI094189-03) and the Johns Hopkins Tuberculosis Research Advancement Center (TRAC) developmental award (P30AI168436). TK was also supported by the Leukemia Research Foundation. SP was also supported by the Leukemia Lymphoma Society Translation Research Program awards, the American Society of Hematology Scholar Award, and the Swim Across America Translational Cancer Research Award. This work was supported by NIH grants: K08AI174959 (SK), K08HL168777 (TK), K08CA270403 (SP), R01AI148710 (PCK), K24AI143447 (PCK), P30AI168436 (PCK). The content is solely the responsibility of the authors and does not necessarily represent the official views of the National Institutes of Health. SK was also supported by the Johns Hopkins CFAR developmental award (5P30AI094189-03) and the Johns Hopkins Tuberculosis Research Advancement Center (TRAC) developmental award (P30AI168436). TK was also supported by the Leukemia Research Foundation. SP was also supported by the Leukemia Lymphoma Society Translation Research Program awards, the American Society of Hematology Scholar Award, and the Swim Across America Translational Cancer Research Award.

Acknowledgments

The content of this publication is available online on the Biorxiv preprint server. Illustrations were created with BioRender.com.

Conflict of interest

Johns Hopkins University has filed patent applications related to technologies described in this paper, of which authors SP, TK, and SK are listed as inventors. Additional patent applications on the work described in this paper may be filed by Johns Hopkins University. The terms of all of these arrangements are being managed by Johns Hopkins University according to its conflict of interest policies. Author SP is a consultant to Merck, owns equity in Gilead and received payment from IQVIA and Curio Sciences.

The remaining authors declare that the research was conducted in the absence of any commercial or financial relationships that could be construed as a potential conflict of interest.

The author(s) declared that they were an editorial board member of Frontiers, at the time of submission. This had no impact on the peer review process and the final decision.

Publisher's note

Supplementary material

The Supplementary Material for this article can be found online at: https://www.frontiersin.org/articles/10.3389/fimmu.2025.1501329/full#supplementary-material

SUPPLEMENTARY FIGURE 1
(A) CD11b+ and CD14+ expression (measured as MFI through flow cytometry) were used to confirm differentiation of THP-1 into macrophages treated with PMA **(B)** THP-1 cells were infected with the GFP+ Mtb strain at MOI of 1 and 10 following treatment with PMA to induce differentiation to macrophages and were incubated for 1 day. Using flow cytometry, CCRL2 expression (MFI) was measured across the different conditions. These experiments were repeated three times, and one-way analysis of variance followed by Tukey's multiple comparisons tests was used; **(C)** populations (%) of cDCs, alveolar macrophages, and neutrophils derived from mouse lungs collected from Mtb-infected vs. uninfected mice; Flow cytometry experiments was repeated at least twice and unpaired T-test was used; MOI, Multiplicity of infection; GFP, green fluorescent protein; D2, Day 2; MFI, Median fluorescent intensity; Mtb, Mycobacterium tuberculosis, CFU, colony-forming units; Classical DCs, classical dendritic cells.

SUPPLEMENTARY FIGURE 2
(A) Hydrophobic interaction chromatography (HPLC) of isotype control antibody and isotype control-SG3249 ADC; **(B)** Scatterplot of spleen mycobacterial burden in mice at 7 weeks after RHZE (n=20); **(C)** Mouse body weights (g) at 7 weeks after RHZE initiation (n=20). One-way analysis of variance followed by Tukey's multiple comparisons tests was used; Mtb, Mycobacterium tuberculosis, RHZE, Rifampin-Isoniazid-Pyrazinamide-Ethambutol; ADC, Antibody-drug conjugate; CFU, colony-forming units.

SUPPLEMENTARY FIGURE 3
Two-dimensional gating strategy for flow cytometric identification of **(A)** T-cell-producing cytokines, **(B)** DCs, alveolar macrophages, and neutrophils. We excluded doublets and debris and gated on single live cells. **(A)** We identified T cells (CD3+), CD4+ T cells, CD8+ T cells, and T-cell producing cytokines (CD3+CD4+ IFN-γ+, or IL-17A+ and CD3+CD8+ IFN-γ+, or IL-17A+); **(B)** classical DCs (CD3-CD19-NK1.1-Ly6G-MHCII+CD11c+) and non-lymphoid tissue cDCs I (CD3-CD19-NK1.1-Ly6G-MHCII+CD11c+CD64-CD103+CD11b-) and cDCs II (CD3-CD19-NK1.1-Ly6G-MHCII+CD11c+CD64-CD103-CD11b+); alveolar macrophages (CD3-CD19-NK1.1-Ly6G-CD11c+CD64+CD11b+); and neutrophils (CD3-CD19-NK1.1-Ly6G+CD11b+); DCs, total classical dendritic cells; cDCs I, classical dendritic cells type I; cDCs II, classical dendritic cells type II.

References

1. WHO. *Tuberculosis* (2023). Available online at: https://www.who.int/news-room/fact-sheets/detail/tuberculosis (Accessed July 22, 2024 2023).

2. Fauci AS. Multidrug-resistant and extensively drug-resistant tuberculosis: the National Institute of Allergy and Infectious Diseases Research agenda and recommendations for priority research. *J Infect Dis*. (2008) 197:1493–8. doi: 10.1086/587904

3. Chuang YM, Dutta NK, Gordy JT, Campodónico VL, Pinn ML, Markham RB, et al. Antibiotic treatment shapes the antigenic environment during chronic TB infection, offering novel targets for therapeutic vaccination. *Front Immunol*. (2020) 11:680. doi: 10.3389/fimmu.2020.00680

4. Kaufmann SHE, Dorhoi A, Hotchkiss RS, Bartenschlager R. Host-directed therapies for bacterial and viral infections. *Nat Rev Drug Discov*. (2018) 17:35–56. doi: 10.1038/nrd.2017.162

5. Young C, Walzl G, Du Plessis N. Therapeutic host-directed strategies to improve outcome in tuberculosis. *Mucosal Immunol*. (2020) 13:190–204. doi: 10.1038/s41385-019-0226-5

6. Fulton SA, Reba SM, Martin TD, Boom WH. Neutrophil-mediated mycobacteriocidal immunity in the lung during Mycobacterium bovis BCG infection in C57BL/6 mice. *Infect Immun*. (2002) 70:5322–7. doi: 10.1128/IAI.70.9.5322-5327.2002

7. Eruslanov EB, Lyadova IV, Kondratieva TK, Majorov KB, Scheglov IV, Orlova MO, et al. Neutrophil responses to Mycobacterium tuberculosis infection in genetically susceptible and resistant mice. *Infect Immun*. (2005) 73:1744–53. doi: 10.1128/IAI.73.3.1744-1753.2005

8. Liu CH, Liu H, Ge B. Innate immunity in tuberculosis: host defense vs pathogen evasion. *Cell Mol Immunol*. (2017) 14:963–75. doi: 10.1038/cmi.2017.88

9. Lee WL, Downey GP. Neutrophil activation and acute lung injury. *Curr Opin Crit Care*. (2001) 7:1–7. doi: 10.1097/00075198-200102000-00001

10. Guirado E, Schlesinger LS, Kaplan G. Macrophages in tuberculosis: friend or foe. *Semin Immunopathol*. (2013) 35:563–83. doi: 10.1007/s00281-013-0388-2

11. Mihret A. The role of dendritic cells in Mycobacterium tuberculosis infection. *Virulence*. (2012) 3:654–9. doi: 10.4161/viru.22586

12. Magallanes-Puebla A, Espinosa-Cueto P, López-Marín LM, Mancilla R. Mycobacterial glycolipid Di-O-acyl trehalose promotes a tolerogenic profile in dendritic cells. *PloS One*. (2018) 13:e0207202. doi: 10.1371/journal.pone.0207202

13. Fujie K, Shinguh Y, Inamura N, Yasumitsu R, Okamoto M, Okuhara M. Release of neutrophil elastase and its role in tissue injury in acute inflammation: effect of the elastase inhibitor, FR134043. *Eur J Pharmacol*. (1999) 374:117–25. doi: 10.1016/S0014-2999(99)00268-X

14. Schioppa T, Sozio F, Barbazza I, Scutera S, Bosisio D, Sozzani S, et al. Molecular basis for CCRL2 regulation of leukocyte migration. *Front Cell Dev Biol*. (2020) 8:615031. doi: 10.3389/fcell.2020.615031

15. Del Prete A, Martínez-Muñoz L, Mazzon C, Toffali L, Sozio F, Za L, et al. The atypical receptor CCRL2 is required for CXCR2-dependent neutrophil recruitment and tissue damage. *Blood*. (2017) 130:1223–34. doi: 10.1182/blood-2017-04-777680

16. Karantanos T, Teodorescu P, Perkins B, Christodoulou I, Esteb C, Varadhan R, et al. The role of the atypical chemokine receptor CCRL2 in myelodysplastic syndrome and secondary acute myeloid leukemia. *Sci Adv*. (2022) 8:eabl8952. doi: 10.1126/sciadv.abl8952

17. Karantanos T, Teodorescu P, Arvanitis M, Perkins B, Jain T, Dezern AE, et al. CCRL2 affects the sensitivity of myelodysplastic syndrome and secondary acute myeloid leukemia cells to azacitidine. *Haematologica*. (2023) 108:1886–99. doi: 10.3324/haematol.2022.281444

18. Petrilli JD, Araújo LE, Da Silva LS, Laus AC, Müller I, Reis RM, et al. Whole blood mRNA expression-based targets to discriminate active tuberculosis from latent infection and other pulmonary diseases. *Sci Rep*. (2020) 10:22072. doi: 10.1038/s41598-020-78793-2

19. Zhang Y, Li S, Liu Q, Long R, Feng J, Qin H, et al. Mycobacterium tuberculosis heat-shock protein 16.3 induces macrophage M2 polarization through CCRL2/CX3CR1. *Inflammation*. (2020) 43:487–506. doi: 10.1007/s10753-019-01132-9

20. Karanika S, Gordy JT, Neupane P, Karantanos T, Ruelas Castillo J, Quijada D, et al. An intranasal stringent response vaccine targeting dendritic cells as a novel adjunctive therapy against tuberculosis. *Front Immunol*. (2022) 13. doi: 10.3389/fimmu.2022.972266

21. Paul S, Pearlman AH, Douglass J, Mog BJ, Hsiue EH, Hwang MS, et al. TCR β chain-directed bispecific antibodies for the treatment of T cell cancers. *Sci Transl Med*. (2021) 13:eabd3595. doi: 10.1126/scitranslmed.abd3595

22. Nichakawade TD, Ge J, Mog BJ, Lee BS, Pearlman AH, Hwang MS, et al. TRBC1-targeting antibody-drug conjugates for the treatment of T cell cancers. *Nature*. (2024) 628:416–23. doi: 10.1038/s41586-024-07233-2

23. Williams KN, Brickner SJ, Stover CK, Zhu T, Ogden A, Tasneen R, et al. Addition of PNU-100480 to first-line drugs shortens the time needed to cure murine tuberculosis. *Am J Respir Crit Care Med*. (2009) 180:371–6. doi: 10.1164/rccm.200904-0611OC

24. Khader SA, Bell GK, Pearl JE, Fountain JJ, Rangel-Moreno J, Cilley GE, et al. IL-23 and IL-17 in the establishment of protective pulmonary CD4+ T cell responses after vaccination and during Mycobacterium tuberculosis challenge. *Nat Immunol*. (2007) 8:369–77. doi: 10.1038/ni1449

25. Cooper AM. Cell-mediated immune responses in tuberculosis. *Annu Rev Immunol*. (2009) 27:393–422. doi: 10.1146/annurev.immunol.021908.132703

26. Darrah PA, Zeppa JJ, Maiello P, Hackney JA, Wadsworth MH, Hughes TK, et al. Prevention of tuberculosis in macaques after intravenous BCG immunization. *Nature*. (2020) 577:95–102. doi: 10.1038/s41586-019-1817-8

27. Karanika S, Wang T, Yilma A, Castillo JR, Gordy JT, Bailey H, et al. Therapeutic DNA vaccine targeting *mycobacterium tuberculosis* persisters shortens curative tuberculosis treatment. *bioRxiv*. (2024). doi: 10.1101/2024.09.03.611055

28. Mellado M, Rodríguez-Frade JM, Vila-Coro AJ, Fernández S, Martín De Ana A, Jones DR, et al. Chemokine receptor homo- or heterodimerization activates distinct signaling pathways. *EMBO J*. (2001) 20:2497–507. doi: 10.1093/emboj/20.10.2497

29. Martínez-Muñoz L, Villares R, Rodríguez-Fernández JL, Rodríguez-Frade JM, Mellado M. Remodeling our concept of chemokine receptor function: From monomers to oligomers. *J Leukocyte Biol*. (2018) 104:323–31. doi: 10.1002/JLB.2MR1217-503R

30. Regan-Komito D, Valaris S, Kapellos TS, Recio C, Taylor L, Greaves DR, et al. Absence of the non-signalling chemerin receptor CCRL2 exacerbates acute inflammatory responses *in vivo*. *Front Immunol*. (2017) 8. doi: 10.3389/fimmu.2017.01621

31. Galligan CL, Matsuyama W, Matsukawa A, Mizuta H, Hodge DR, Howard OM, et al. Up-regulated expression and activation of the orphan chemokine receptor, CCRL2, in rheumatoid arthritis. *Arthritis Rheum*. (2004) 50:1806–14. doi: 10.1002/art.20275

32. Lambrecht BN. Dendritic cells and the regulation of the allergic immune response. *Allergy*. (2005) 60:271–82. doi: 10.1111/j.1398-9995.2005.00708.x

33. Otero K, Vecchi A, Hirsch E, Kearley J, Vermi W, Del Prete A, et al. Nonredundant role of CCRL2 in lung dendritic cell trafficking. *Blood*. (2010) 116:2942–9. doi: 10.1182/blood-2009-12-259903

34. Ogitani Y, Aida T, Hagihara K, Yamaguchi J, Ishii C, Harada N, et al. DS-8201a, A novel HER2-targeting ADC with a novel DNA topoisomerase I inhibitor, demonstrates a promising antitumor efficacy with differentiation from T-DM1. *Clin Cancer Res*. (2016) 22:5097–108. doi: 10.1158/1078-0432.CCR-15-2822

35. Zammarchi F, Corbett S, Adams L, Tyrer PC, Kiakos K, Janghra N, et al. ADCT-402, a PBD dimer–containing antibody drug conjugate targeting CD19-expressing Malignancies. *Blood*. (2018) 131:1094–105. doi: 10.1182/blood-2017-10-813493

36. Paul S, Konig MF, Pardoll DM, Bettegowda C, Papadopoulos N, Wright KM, et al. Cancer therapy with antibodies. *Nat Rev Cancer*. (2024) 24:399–426. doi: 10.1038/s41568-024-00690-x

37. Monnier J, Lewén S, O'hara E, Huang K, Tu H, Butcher EC, et al. Expression, regulation, and function of atypical chemerin receptor CCRL2 on endothelial cells. *J Immunol*. (2012) 189:956–67. doi: 10.4049/jimmunol.1102871

38. Xu M, Wang YM, Li WQ, Huang CL, Li J, Xie WH, et al. Ccrl2 deficiency deteriorates obesity and insulin resistance through increasing adipose tissue macrophages infiltration. *Genes Dis*. (2022) 9:429–42. doi: 10.1016/j.gendis.2020.08.009

39. Lowe DM, Bandara AK, Packe GE, Barker RD, Wilkinson RJ, Griffiths CJ, et al. Neutrophilia independently predicts death in tuberculosis. *Eur Respir J*. (2013) 42:1752–7. doi: 10.1183/09031936.00140913

40. De Melo MGM, Mesquita EDD, Oliveira MM, Da Silva-Monteiro C, Silveira AKA, Malaquias TS, et al. Imbalance of NET and alpha-1-antitrypsin in tuberculosis patients is related with hyper inflammation and severe lung tissue damage. *Front Immunol*. (2018) 9:3147. doi: 10.3389/fimmu.2018.03147